

# TRIM3 inhibits colorectal cancer cell migration and lipid droplet formation by promoting FABP4 degradation

Qi Zuo<sup>1</sup>, Qimei Xu<sup>2</sup>, Zhen Li<sup>2</sup>, Dixian Luo<sup>3</sup>, Hanwu Peng<sup>1</sup> and Zhi Duan<sup>2</sup>

<sup>1</sup>Department of Emergency, <sup>2</sup>Department of Pathology, The First Hospital of Changsha, Changsha, Hunan and <sup>3</sup>Department of Laboratory Medicine, Huazhong University of Science and Technology Union Shenzhen Hospital, Shenzhen, Guangdong, PR China

**Summary.** This study is to investigate the regulation of TRIM3/FABP4 on colorectal cancer (CRC) cell migration and lipid metabolism. After transfection of HCT116, LoVo, or SW480 cells, the expression of FABP4, TRIM3, N-cadherin, Vimentin, E-cadherin, and lipid droplet (LD) formation-related genes was measured by qRT-PCR or western blot assays. Wound healing and Transwell assays were applied to detect CRC cell migration and invasion abilities. The levels of triglyceride (TG) and total cholesterol (TC) were measured and the formation of LDs was observed. Additionally, the relationship between FABP4 and TRIM3 was confirmed by Co-IP and ubiquitination assays. Furthermore, a liver metastasis model of CRC was established to explore the effect of FABP4 on CRC tumor metastasis *in vivo*. FABP4 was upregulated in CRC cells. Downregulation of FABP4 or upregulation of TRIM3 resulted in repressed cell migration and invasion, decreased TG and TC levels, and reduced numbers of LDs. In nude mice, knockdown of FABP4 reduced metastatic nodules in the liver. Mechanistically, TRIM3 combined FABP4 and decreased its protein expression by ubiquitination. Overexpressed FABP4 reversed the influence of TRIM3 upregulation on CRC cell migration and LD formation. In conclusion, underexpressed TRIM3 suppressed FABP4 ubiquitination and accelerated CRC cell migration and LD formation.

**Key words:** Colorectal cancer, FABP4, TRIM3, Ubiquitination, Lipid droplet, Metastasis

## Introduction

Colorectal cancer (CRC) is one of the most common primary malignancies in the digestive system possessing high incidence and fatality rates in both sexes (Siegel et

al., 2021). Because the symptoms of CRC in the early stage are not obvious, most patients are in an advanced stage at the time of diagnosis (Dekker et al., 2019). Although the therapeutic strategies for CRC have evolved considerably over the past years, including surgery, chemotherapy, radiotherapy, and immunotherapy (Chen et al., 2021b), the prognosis of patients with CRC remains dismal. Tumor metastasis is the leading cause of death in most cancer patients, which has been regarded as the major obstacle in the treatment and prognosis of CRC (Zhang et al., 2021a; Jia et al., 2022). Hence, a study of the molecular mechanisms regulating tumor metastasis assumes great significance for the treatment of patients with CRC.

Fatty acid binding proteins (FABPs), a member of the intracellular lipid binding protein superfamily, can regulate lipid trafficking and metabolism by binding to hydrophobic ligands (Sun and Zhao, 2022). As the most characteristic and most studied protein in the FABPs family, FABP4 is highly expressed in adipocytes and regarded as one of the markers for identifying adipocytes (Mandl et al., 2022). Also, FABP4 has been detected to be strongly expressed in many malignant solid tumors such as CRC (Zhang et al., 2019), breast cancer (Tsakogiannis et al., 2021), prostate cancer (Huang et al., 2017a), ovarian cancer (Baczewska et al., 2022), etc., and serves as a tumor-promoting molecule. However, the role of FABP4 in CRC tumor metastasis and its potential molecular regulatory mechanisms have not been elucidated.

Tripartite motif (TRIM) proteins, one of the subfamilies of E3 ubiquitin ligases, are reported to be linked with a variety of biological processes and directly participate in human diseases and cancers (Venuto and Merla, 2019). Among these TRIM members, TRIM3 was often studied as a tumor inhibitor. A study on liver cancer visualized that TRIM3 overexpression could reduce cell viability *in vitro* and repress tumor growth and metastasis *in vivo* (Huang et al., 2017b). Similarly, TRIM3 was found to be underexpressed in breast cancer cells and tissues and have a suppressive effect on breast cancer tumor growth (Li et al., 2019). From the Cancer

Corresponding Author: Zhi Duan, Department of Pathology, The First Hospital of Changsha, No. 311 Yingpan Road, Kaifu District, Changsha, Hunan 410005, PR China. e-mail: duanzhi168@163.com  
www.hh.um.es. DOI: 10.14670/HH-18-627



Genome Atlas (TCGA) analysis and Gene Expression Profiling Interactive Analysis (GEPIA) prediction, TRIM3 was downregulated in colonic adenocarcinoma (COAD) and rectum adenocarcinoma (READ). A previous study showed that TRIM3 played a tumor-suppressive function in CRC progression (Piao et al., 2016). Meanwhile, the analysis of the GEPIA database in our study showed a positive correlation between FABP4 and lipid droplet (LD) formation-related genes including fatty acid synthase (FASN), stearoyl-CoA desaturase (SCD), and acyl-CoA synthetase long chain family member 1 (ACSL1) in COAD and READ. Consequently, we postulated that TRIM3 exerted its role in lipid metabolism and tumor metastasis of CRC through regulating FABP4 protein stability, and then conducted a series of experiments to verify this hypothesis, intending to provide a new molecular direction for CRC treatment.

## Materials and methods

### Cell culture and transfection

CRC cell lines (HCT116, LoVo, SW480, and HT-29) and a normal colonic epithelial cell line (NCM460) were obtained from American Type Culture Collection cell bank (ATCC; Manassas, VA, USA). All cells were stored in Dulbecco's modified Eagle medium (DMEM; Gibco, USA) appended with 10% fetal bovine serum (Gibco) at 37°C under a 5% CO<sub>2</sub> atmosphere.

FABP4 knockdown vector (sh-FABP4), FABP4 and TRIM3 overexpression vectors (oe-FABP4 and oe-TRIM3), and their negative controls (sh-NC and oe-NCs) were purchased from GeneChem (Shanghai, China). Cell transfection was performed based on the instruction on a Lipofectamine 2000 kit (Invitrogen, Carlsbad, CA, USA). Follow-up experiments were conducted after transfection for 48h.

### TCGA analysis

TCGA combined with Genotype-Tissue Expression Project (GTEx) method was adopted for analyzing differentially expressed genes (DEGs) in CRC. The Genomic Data Commons (GDC)-TCGA READ and COAD files in HTSeq-FPKM format were downloaded from the TCGA database (<https://xenabrowser.net/datapages/>), and the mRNA transcriptome data of READ and COAD were analyzed through R studio. Meanwhile, the mRNA transcriptome data of normal tissues corresponding to cancer tissues were extracted from the GTEx database. Subsequently, the above-collected data in the mRNA expression matrix were analyzed by limma package with  $|\log_{2}FC| > 1$  and Adjust  $P < 0.05$  as standard screening thresholds. Finally, a volcano plot was made by SangerBox online website (<http://sangerbox.com/Tool>) to display the screened DEGs.

### GEPIA

The GEPIA database (<http://gepia.cancer-pku.cn/detail.php>) was used to assess the correlation (Pearson correlation analysis) between FABP4 and lipid droplet formation-related genes (FASN, SCD, and ACSL1) in READ and COAD.

### Quantitative reverse transcription polymerase chain reaction (qRT-PCR)

The extraction of total RNA was performed in accordance with the manuals of Trizol (Invitrogen, Carlsbad, CA, USA). After reverse transcription (PrimeScript RT, Takara, Japan), reaction conditions were set based on the protocols of the fluorescent quantitative PCR kit (Takara), and the expression of related genes was detected on an ABI 7500 RT-PCR (ABI, Foster City, CA, USA). Three duplicates were set for each reaction of PCR. GAPDH served as an internal reference and 2<sup>-ΔΔCt</sup> method (ΔΔCt=ΔCt experimental group - ΔCt control group, ΔCt=CT [target gene] - CT [internal reference]) was used to calculate the relative expression of each target gene. Primers are listed in Table 1.

### Western blot assay

Cells were lysed with enhanced protease inhibitor-contained RIPA lysis buffer (Boster Biological Technology Co., Ltd., Wuhan, China), placed on ice for 30 min, and then centrifuged for 10 min (4°C, 12000 rpm). The absorbed supernatant was divided into centrifugation tubes (0.5 mL) and stored at -20°C, or quantified by a BCA kit (Boster). Afterward, the protein was denatured with 6×SDS sample loading buffer at 100°C, followed by electrophoresis and membrane transferring (4°C, 1.5h). Next, the membrane was blocked with 5% skim milk (prepared by TBST) for 1h. Primary antibodies against TRIM3 (sc-136363, Santa Cruz Biotechnology (SCBT), USA), FABP4 (sc-271529, SCBT), E-cadherin (sc-8426, SCBT), Vimentin (sc-6260, SCBT), N-cadherin (sc-8424, SCBT), FASN (ab128870, Abcam, Cambridge, USA), SCD (sc-81776, SCBT),

**Table 1.** Primer sequences used in qRT-PCR analysis.

Name of primer	Sequence (5'-3')
FABP4-F	CTGGCATGGCCAAACCTAAC
FABP4-R	TCCTGGCCCAGTATGAAGGA
TRIM3-F	GCCCCAACCATGAAGACGAT
TRIM3-R	CTGTTTGGCCCCACAAATGG
GAPDH-F	AAGCCTGCCGGTGACTAAC
GAPDH-R	TGGACTCCACGACGTACTCA

F, forward; R, reverse.

## FABP4 promotes CRC cell migration

ACSL1 (ab177958, Abcam), and GAPDH (ab8245, Abcam) were incubated with the membrane overnight at 4°C. TBST washing later (3×10 min), goat anti-rabbit or goat anti-mouse secondary antibody was appended for 2h incubation. After washing and color development, the expression of target proteins was detected.

### Wound healing assay

After inoculation into 6-well plates, the cells with 80% confluence were scratched with a 200 µL pipette tip. The culture medium was replaced with serum-free DMEM. Cells under the same field were photographed at 0 and 24h, and the change of the scratch width was determined by Image J.

### Invasion assay

Cells were digested by trypsin, washed with PBS, and re-suspended in a serum-free medium. A total of 10<sup>5</sup> cells were inoculated on the upper Transwell chamber which was covered with matrigel (200 µL per well). After incubation for 48h, the invaded cells were washed with PBS twice and stained with 0.1% crystal violet, subsequent to microscopic observation.

### Oil red O staining

Cells were seeded onto a 12-well plate, and when they reached a density of 80%, the cells underwent PBS washing thrice and 30-min fixation with 4% paraformaldehyde. After washing, the cells were stained by oil red O solution for 30 min. Under a microscope, the images of red LDs were captured. In addition, the eluted oil red O stain was quantified by measuring the absorbance at 510 nm after being diluted with 100% isopropanol.

### Detection of triglyceride (TG) and total cholesterol (TC)

Cells were cultured in a 12-well plate for 48h and then digested by trypsin. Cell pellets were collected, washed with PBS, and centrifuged. According to the proportion of 100 µL lysis for 10<sup>5</sup> cells, an appropriate amount of lysis in the TG or TC kit was blended with the pellets to lyse cells for 10 min. The supernatant was taken for ELISA after protein quantification based on the instructions of the kit (Applygen, Beijing, China). Finally, the absorbance of each sample at 550 nm was assessed.

### The liver metastasis model of CRC

Twelve female nude mice (BALB/c, 5 weeks old, 20~25 g) were purchased from Shanghai SLAC Laboratory Animal Co., Ltd. (Shanghai, China). Nude mice were randomly assigned into sh-FABP4 (mice were injected with HCT116 cells transfected with sh-FABP4 via spleen) and sh-NC (mice were subjected to HCT116 cells transfected with sh-NC via spleen) groups. Each

group contained six mice.

The animal experiments were conducted based on the National Institutes of Health Laboratory Animal Care and Use Guidelines and the approval of the Ethics Committee of The First Hospital of Changsha. After the mice were anesthetized, the fur was shaved to expose the skin for disinfection. Next, the outer skin was dissected and then the inner muscle layer was dissected with new scissors, after which the long oval reddish-brown spleen was exposed with toothless forceps for injection. Immediately, 100 µL of cell suspension (10<sup>6</sup> cells) was injected into the distal tip of the spleen, subsequent to disinfection and surgical suture. After 30 days, the mice were euthanized, and the liver specimens were collected and examined for metastatic nodules (Li et al., 2021; Liu et al., 2021).

### Co-IP assay

Cells were lysed with pre-cooled RIPA lysis buffer and centrifuged for 15 min (14000 g, 4°C), after which the supernatant was removed to a new tube. Anti-TRIM3 (sc-136363, SCBT) was added into the tube for overnight incubation of the antigen-antibody complex at 4°C on a shaker, and IgG antibody was used as the NC group. Following the addition of 100 µL Protein A/G agarose beads (prepared in PBS with a concentration of 50%), the agarose bead-antigen-antibody complex was obtained after centrifugation (14000 rpm, 5 s). Next, the complex was rinsed thrice with pre-cooled RIPA buffer and suspended with 2×loading buffer. The sample was boiled for 5 min and centrifuged (14000 g) to collect the remaining agarose beads. Protein expression was evaluated via western blot assay.

### Analysis of ubiquitination

Cells were transfected with oe-TRIM3, Myc-FABP4, and HA-ubiquitin (all from Genomeditech, Shanghai, China) using Lipofectamine 2000 (Invitrogen). Next, the cells were treated with 20 µM proteasome inhibitor MG132 for 6h, washed twice with pre-cooled PBS, and then lysed with RIPA lysis buffer. Cytoplasmic proteins obtained from the lysate by centrifugation were incubated with anti-Myc antibody overnight. The antigen-antibody mixture was incubated (4°C, 4h) with 100 µL Protein A/G agarose beads on a shaker, followed by 3 washes of lysis buffer and boiling in 2×SDS loading buffer. The eluted protein was detected by western blot assay with anti-HA antibody (ab9110, Abcam).

### Statistical analysis

Data were analyzed by GraphPad prism8 software and manifested in the form of mean ±standard deviation. Comparisons between two groups were tested by t-test while that among multiples was determined using one-way analysis of variance, with Tukey's multiple

comparisons test as the post hoc analysis.  $P < 0.05$  was considered to have statistical significance.

## Results

### *FABP4 promotes CRC metastasis*

The expression of FABP4 in CRC cell lines (HCT116, LoVo, SW480, and HT-29) was detected by qRT-PCR and western blot assays, and the results showed that the mRNA and protein expression of FABP4 was invisibly elevated in the four CRC cell lines related to the NCM460 cell line (Fig. 1A,B). Among them, FABP4 was expressed relatively stronger in HCT116 and LoVo cell lines, thus these two cell lines were selected for subsequent experiments.

After HCT116 and LoVo cells were transfected with sh-FABP4, the effect of FABP4 on CRC cell migration was investigated. Compared with the sh-NC group, the sh-FABP4 group had reduced FABP4 mRNA and protein expression (Fig. 1C,D), migration rate (Fig. 1E), and invasion capacity (Fig. 1F). As reflected in Figure 1G, the expression of N-cadherin and Vimentin was clearly decreased but the expression of E-cadherin was signally more increased in the sh-FABP4 group than in the sh-NC group. These results demonstrated that knockdown of FABP4 could inhibit CRC cell migration, invasion, and epithelial-mesenchymal transition.

Subsequently, we established a liver metastasis model of CRC to explore the effect of FABP4 on CRC tumor metastasis in vivo. From qRT-PCR and western blot analysis results, the mRNA and protein expression of FABP4 in liver tissues of the sh-FABP4 group was decreased versus the sh-NC group (Fig. 1H,I). In comparison with the control mice, mice injected with HCT116 cells transfected with sh-FABP4 had fewer metastatic nodules in the liver (Fig. 1J).

### *FABP4 facilitates LD formation in CRC cells*

Through GEPIA database analysis, FABP4 was positively correlated with LD formation-related genes FASN, SCD, and ACSL1 in COAD and READ (Fig. 2A), which indicated a close relationship between FABP4 and lipid metabolism in CRC.

Next, we transfected HCT116 and LoVo cells with sh-FABP4 and verified the effect of FABP4 in LD formation through a series of experiments. Revealed by western blot assay, the sh-FABP4 group had lower protein levels of FASN, SCD, and ACSL1 (vs. the sh-NC group) (Fig. 2B). TG and TC levels can indirectly reflect the formation of LDs in cells. Results in Figure 2C,D showed that the TG and TC levels in the sh-FABP4 group were observably reduced (vs. the sh-NC group). From oil red O staining, it was clear that the number of intracellular LDs in the sh-FABP4 group was decreased (vs. the sh-NC group) (Fig. 2E). Taken together, FABP4 had a facilitative effect on LD formation in CRC cells.

### *TRIM3 accelerates FABP4 degradation through ubiquitination*

TCGA analysis demonstrated that TRIM3 was downregulated in COAD and READ (Fig. 3A), which was also confirmed through GEPIA database analysis (Fig. 3B). On account of the above predictions, we speculated that TRIM3 may play a role in the regulation of FABP4 protein stability in CRC. Consistently, our data revealed that TRIM3 was expressed modestly in HCT116 and LoVo cells versus NCM460 cells (Fig. 3C,D).

To investigate the effect of TRIM3 on the stability of FABP4 protein, we transfected oe-TRIM3 into HCT116 and LoVo cells and conducted a series of experiments. Western blot and qRT-PCR assays demonstrated that overexpression of TRIM3 did not affect FABP4 mRNA level (Fig. 3E) but inhibited its protein expression (Fig. 3F). Displayed by Co-IP, TRIM3 antibody aggregated FABP4 protein (Fig. 3G). As reflected in Figure 3H, overexpressed TRIM3 strongly promoted FABP4 ubiquitination in the presence of MG132 (an effective 26S proteasome inhibitor). The above results suggested that TRIM3 may repress FABP4 protein level via ubiquitination.

### *TRIM3 represses cell migration and LD formation via FABP4 downregulation*

Finally, HCT116 and LoVo cells experienced transfection with oe-TRIM3 or oe-TRIM3 + oe-FABP4. Relatedly, oe-TRIM3 + oe-NC group had elevated TRIM3 mRNA and protein expression and reduced FABP4 protein (vs. oe-NC + oe-NC group); the mRNA and protein expression of FABP4 was visibly increased but TRIM3 expression had no change in oe-TRIM3 + oe-FABP4 group (vs. the oe-TRIM3 + oe-NC group) (Fig. 4A,B).

In HCT116 and LoVo cells, cell migration and invasion were evaluated by wound healing and Transwell assays. The protein expression of epithelial-mesenchymal transition- and lipid metabolism-related genes was detected by western blot assay. TG and TC levels were tested by kits. The formation of LD was observed through oil red O staining. In comparison with the oe-NC + oe-NC group, HCT116 and LoVo cell abilities of migration and invasion were inhibited in the oe-TRIM3 + oe-NC group (Fig. 4C,D). The expression of N-cadherin and Vimentin was clearly decreased but E-cadherin expression was increased in the oe-TRIM3 + oe-NC group (vs. the oe-NC + oe-NC group) (Fig. 5A). Moreover, the oe-TRIM3 + oe-NC group had reduced levels of FASN, SCD, ACSL1, TG, and TC versus the oe-NC + oe-NC group (Fig. 5B-D). The number of intracellular LDs was markedly diminished in HCT116 and LoVo cells of the oe-TRIM3 + oe-NC group (vs. the oe-NC + oe-NC group) (Fig. 5E), whereas, co-transfection of oe-TRIM3 and oe-FABP4 reversed the effect of oe-TRIM3 alone on HCT116 and LoVo cell

## FABP4 promotes CRC cell migration

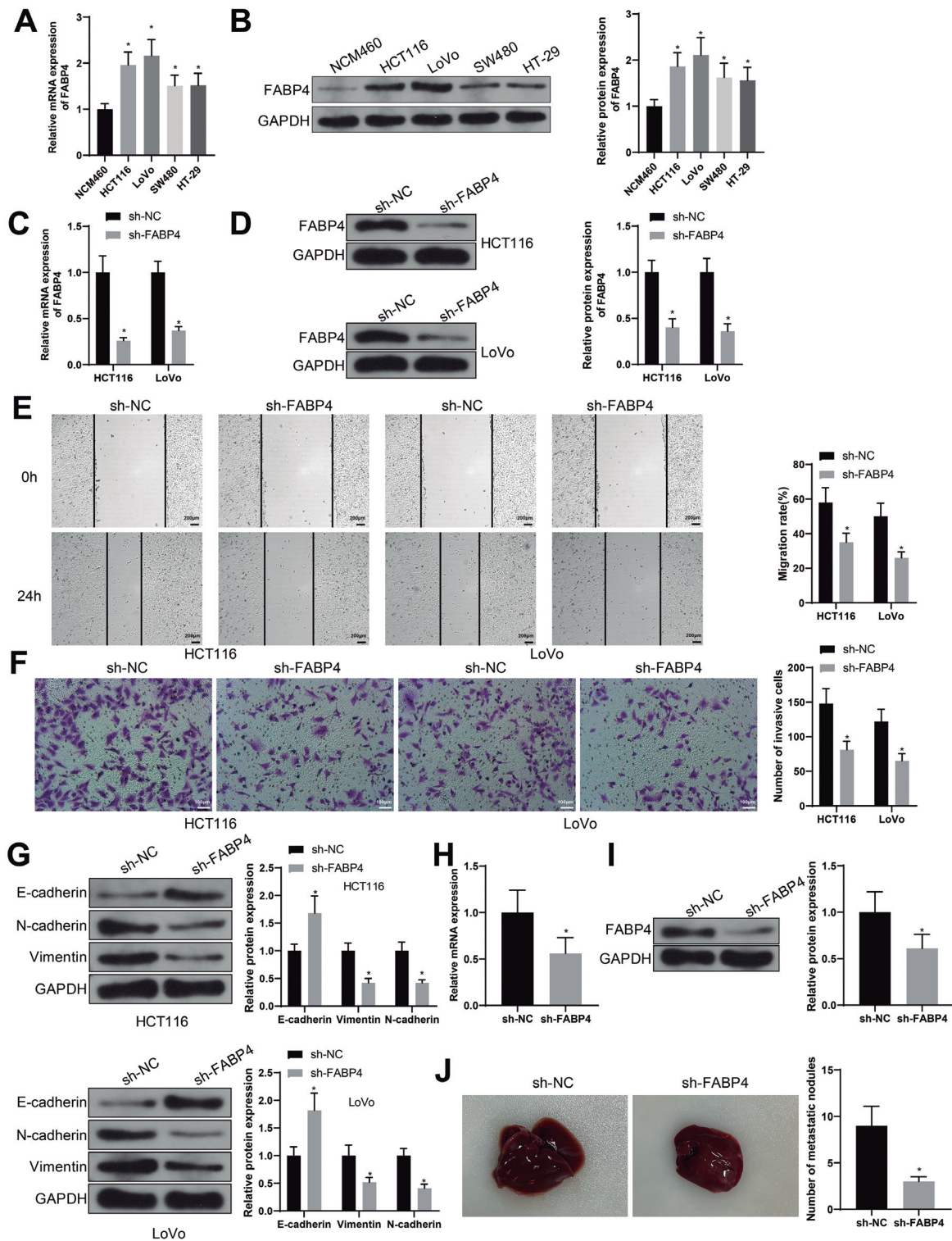


**Fig. 1.** FABP4 facilitates CRC metastasis *in vitro* and *in vivo*. **A.** The mRNA expression of FABP4 was detected by qRT-PCR. **B.** The protein expression of FABP4 was detected by western blot assay. After HCT116 and LoVo cells were transfected with sh-FABP4. **C.** The mRNA expression of FABP4 was tested by qRT-PCR. **D.** The protein expression of FABP4 was tested by western blot assay. **E.** Cell migration was assessed by wound healing assay. **F.** Cell invasion was assessed by Transwell assay. **G.** The expression of N-cadherin, Vimentin, and E-cadherin was examined by western blot assay. After the liver metastasis model of CRC was established. **H.** The mRNA expression of FABP4 was evaluated by qRT-PCR. **I.** The protein expression of FABP4 was evaluated by western blot assay. **J.** The metastatic nodules in the liver were observed. Data were expressed as mean  $\pm$  standard deviation. T-test and one-way analysis of variance were used for comparisons between two groups and among groups, respectively. Tukey's multiple comparisons test was used for post hoc analysis. Each cellular experiment was repeated thrice. Animal experiment, N=6. \*,  $P < 0.05$ . CRC, colorectal cancer.

## FABP4 promotes CRC cell migration

functions.

Similarly, SW480 cells were transfected with oe-TRIM3 or oe-TRIM3 + oe-FABP4, followed by a series of functional experiments after successful transfection

(Fig. 6A,B). Versus the oe-NC + oe-NC group, SW480 cell migration and invasion were inhibited in the oe-TRIM3 + oe-NC group, accompanied by reductions in the protein levels of FASN, SCD, and ACSL1, the levels

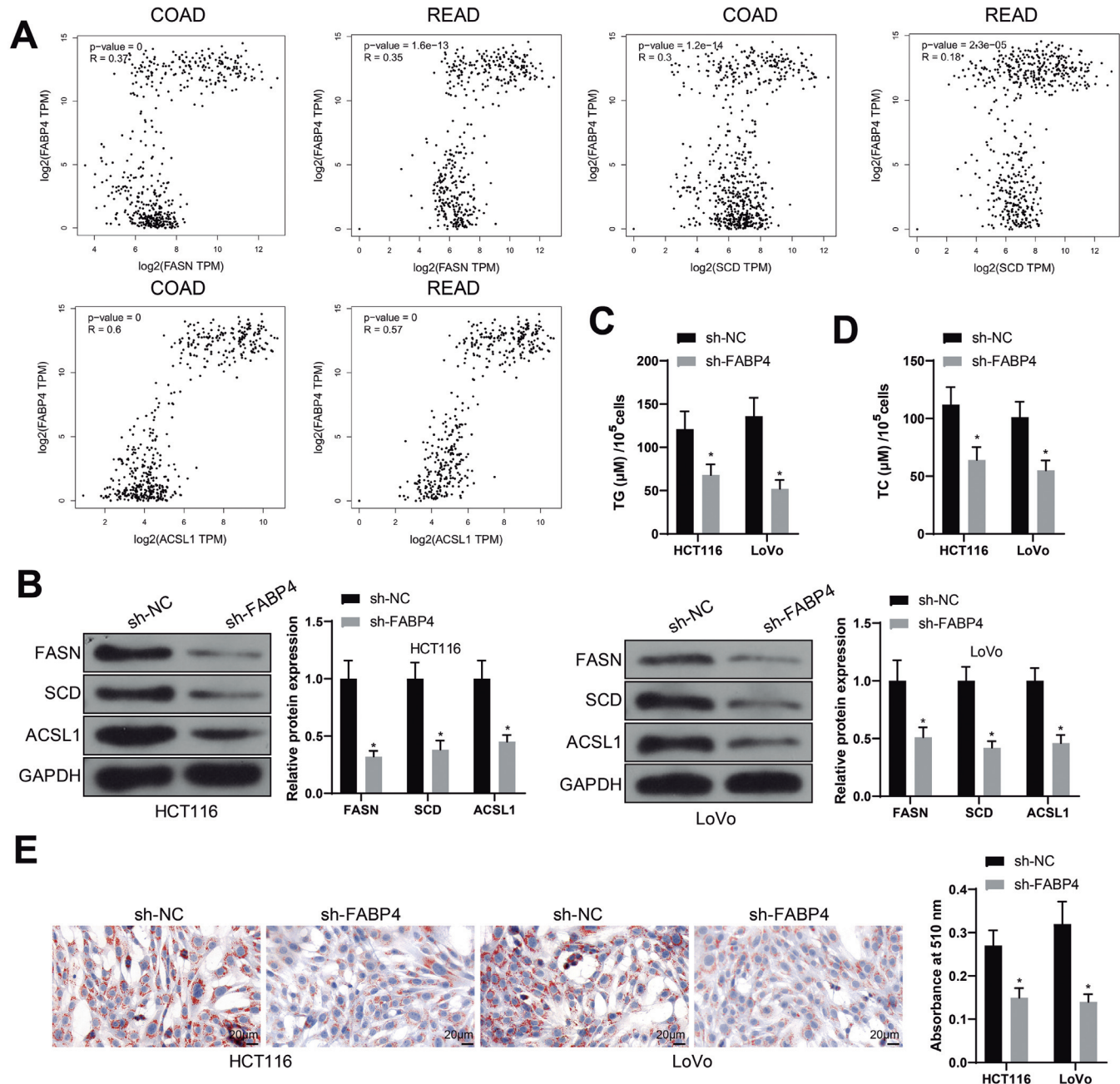


**Fig. 2.** FABP4 promotes the formation of LD in CRC cells. **A.** The correlation between FABP4 and LD formation-related genes (FASN, SCD, and ACSL1) in COAD and READ was predicted by GEPIA database. After HCT116 and LoVo cells were transfected with sh-FABP4. **B.** The protein levels of FASN, SCD, and ACSL1 were assessed by western blot assay. **C, D.** The levels of TG and TC were tested by ELISA kits. **E.** The number of intracellular LDs was observed through oil red O staining. Data were expressed as mean  $\pm$  standard deviation, and t-test was used for comparisons between two groups. Each cellular experiment was repeated three times. \*,  $P < 0.05$ . CRC, colorectal cancer; FASN, fatty acid synthase; SCD, stearyl-CoA desaturase; ACSL1, acyl-CoA synthetase long chain family member 1; TG, triglyceride; TC, total cholesterol; COAD, colonic adenocarcinoma; READ, rectum adenocarcinoma; LD, lipid droplet.

## FABP4 promotes CRC cell migration

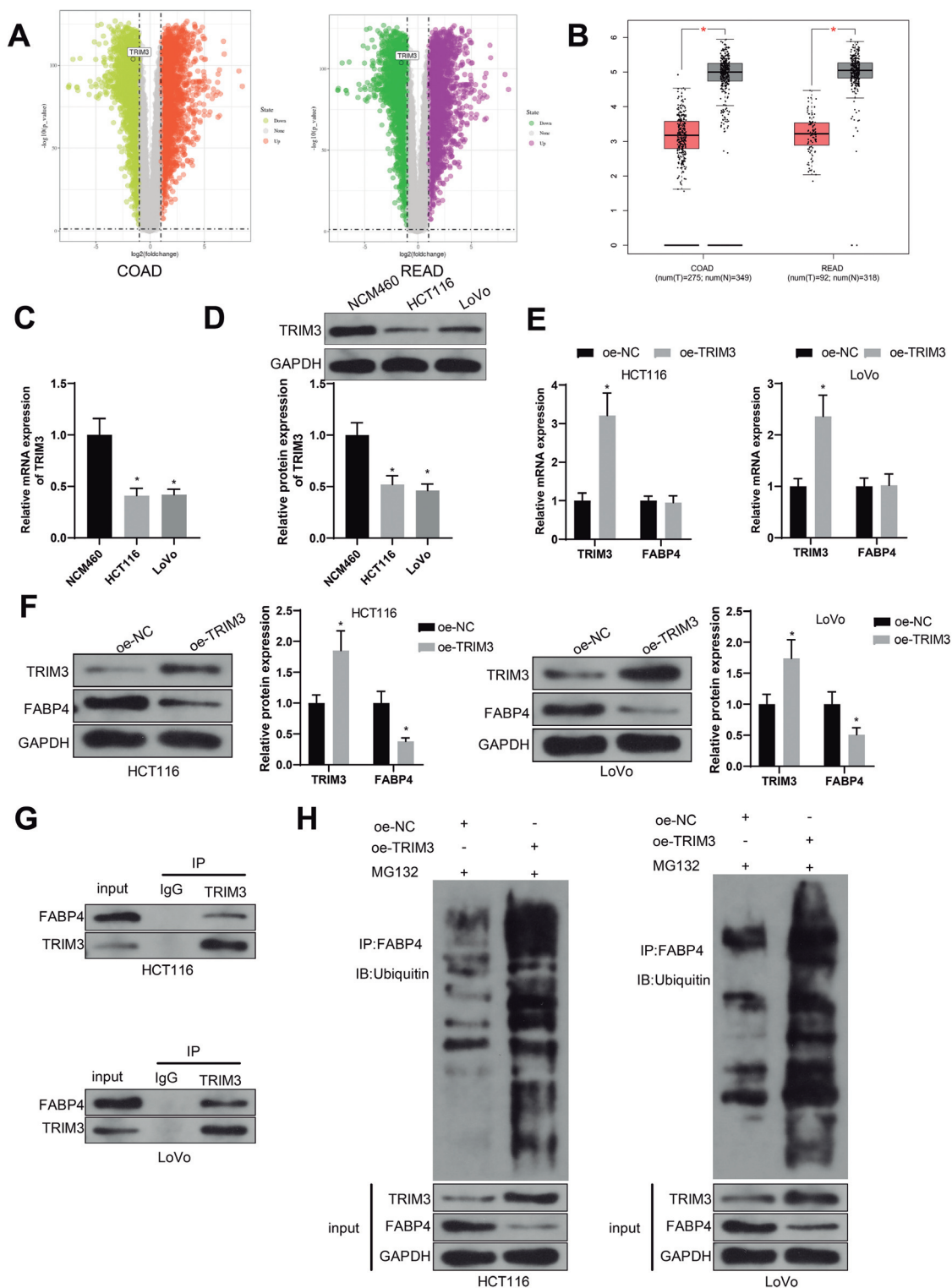


**Fig. 3.** TRIM3 inhibits FABP4 protein level by ubiquitination. **A.** The expression of TRIM3 in COAD and READ was analyzed by TCGA. **B.** The expression of TRIM3 in COAD and READ was predicted by GEPIA database. **C.** TRIM3 mRNA level in HCT116 and LoVo cells was detected by qRT-PCR. **D.** The protein expression of TRIM3 in HCT116 and LoVo cells was tested by western blot assay. After HCT116 and LoVo cells were transfected with oe-TRIM3. **E.** TRIM3 and FABP4 mRNA levels were measured by qRT-PCR. **F.** The protein expression of TRIM3 and FABP4 was measured by western blot assay. **G.** Co-IP assay was used to detect the interaction of TRIM3 and FABP4. **H.** The ubiquitination level of FABP4 was assessed by western blot assay. Data were shown in the form of mean  $\pm$  standard deviation. T-test and one-way analysis of variance were used for comparisons between two groups and among groups, respectively. Tukey's multiple comparisons test was used for post hoc analysis. All assays were repeated thrice. \*,  $P < 0.05$ . CRC, colorectal cancer; COAD, colonic adenocarcinoma; READ, rectum adenocarcinoma.

## FABP4 promotes CRC cell migration

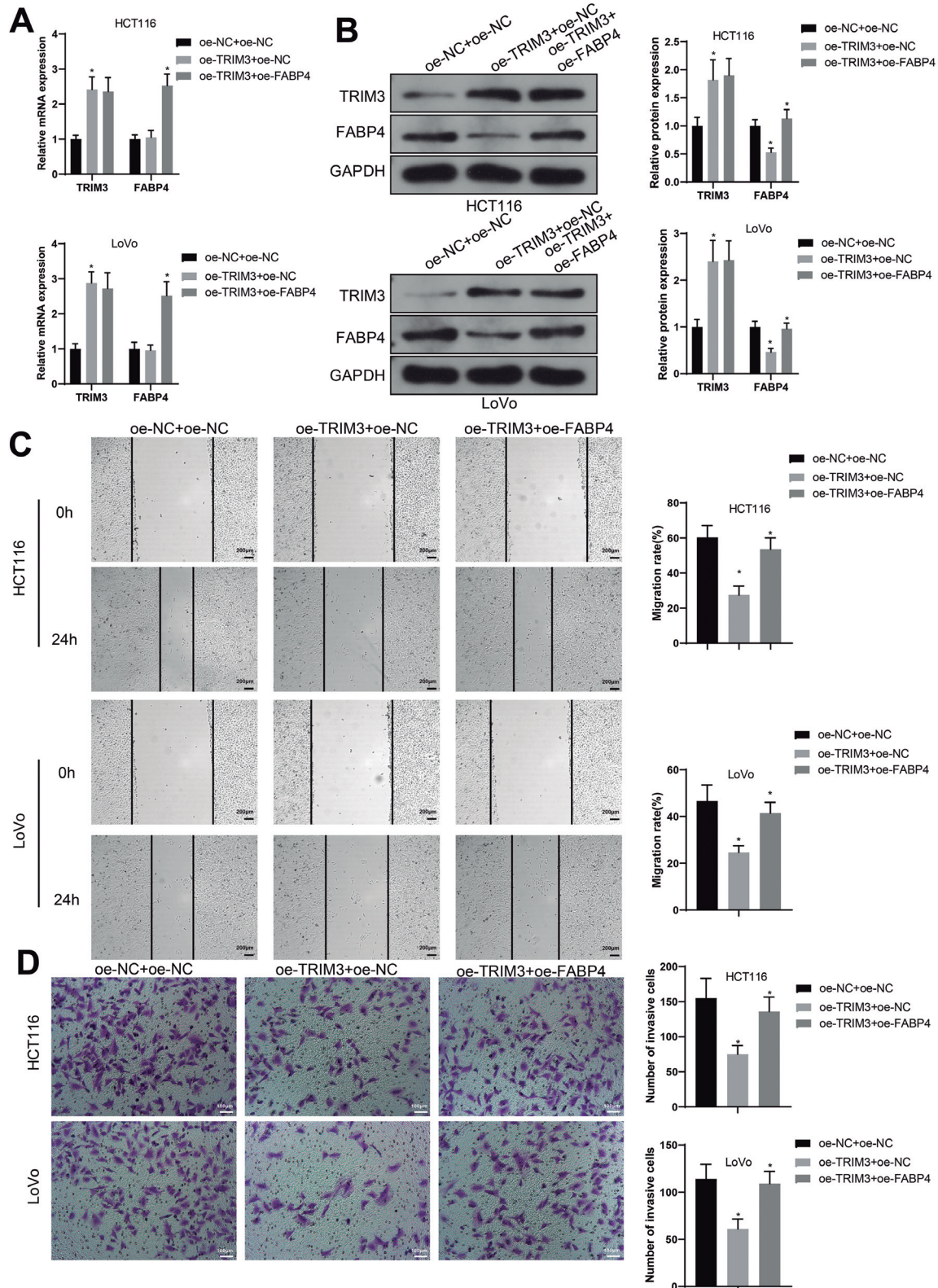


**Fig. 4.** TRIM3 regulates the migration of HCT116 and LoVo cells via FABP4. After HCT116 and LoVo cells were transfected with oe-TRIM3 or co-transfected with oe-TRIM3 and oe-FABP4. **A.** The mRNA levels of TRIM3 and FABP4 were detected by qRT-PCR. **B.** The protein expression of TRIM3 and FABP4 was detected by western blot assay. **C.** Cell migration was tested using wound healing assay. **D.** Cell invasion was tested using Transwell assay. Data were shown in the form of mean  $\pm$  standard deviation. One-way analysis of variance was used for comparisons among groups, and Tukey's multiple comparisons test was used for post hoc analysis. All assays were repeated thrice. \*,  $P < 0.05$ . CRC, colorectal cancer.

## FABP4 promotes CRC cell migration

of TG, and TC, and the number of intracellular LDs (Fig. 6C-H). Nevertheless, co-transfection of oe-TRIM3 and oe-FABP4 reversed the effect of oe-TRIM3 alone on SW480 cell functions.

In summary, TRIM3 regulated CRC cell migration and LD formation via FABP4.

## Discussion

LD is an important organelle for fat storage in the

body, and its dynamic regulation can affect the energy metabolism homeostasis of the whole body (Walther et al., 2017). Additionally, the energy provided by cancer cells through fatty acids promotes tumor development and metastasis (Fujii et al., 2017). A prior study suggested that overproduction of LD facilitated CRC cell metastasis, implicating its potential use as a prognostic biomarker for CRC recurrence and survival (Li et al., 2020). Therefore, in the present study, we researched the regulatory factors and mechanisms that

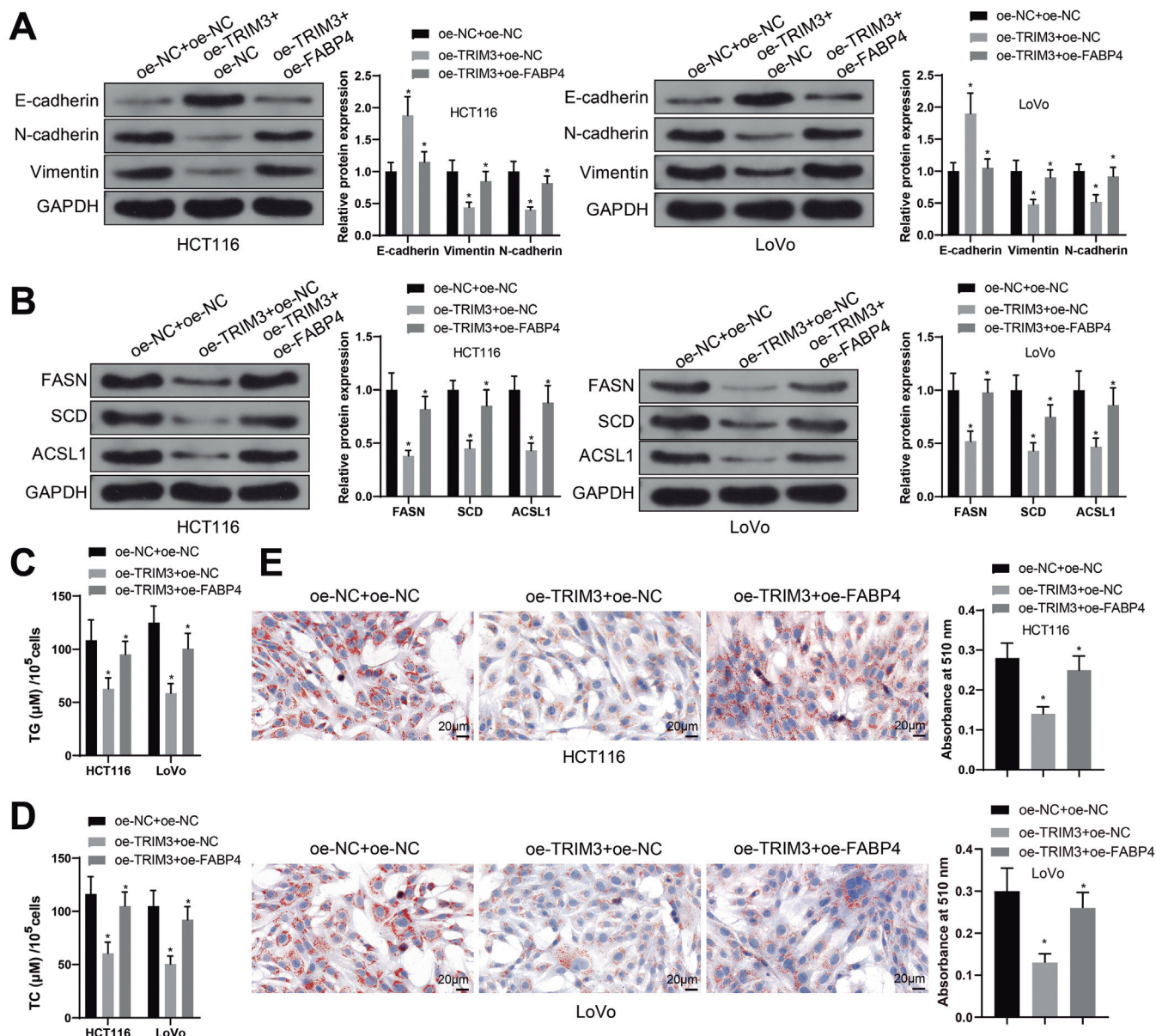


**Fig. 5.** TRIM3 regulates the formation of LD in HCT116 and LoVo cells via FABP4. **A.** The expression of N-cadherin, Vimentin, and E-cadherin was examined by western blot assay. **B.** The protein levels of FASN, SCD, and ACSL1 were assessed by western blot assay. **C, D.** The levels of TG and TC were tested by ELISA kits. **E.** The number of intracellular LDs was observed through oil red O staining. All data were exhibited as mean  $\pm$  standard deviation. One-way analysis of variance was used for comparisons among groups, and Tukey's multiple comparisons test was used for post hoc analysis. All experiments were performed thrice. \*,  $P < 0.05$ . CRC, colorectal cancer; FASN, fatty acid synthase; SCD, stearoyl-CoA desaturase; ACSL1, acyl-CoA synthetase long chain family member 1; TG, triglyceride; TC, total cholesterol; LD, lipid droplet.

## FABP4 promotes CRC cell migration

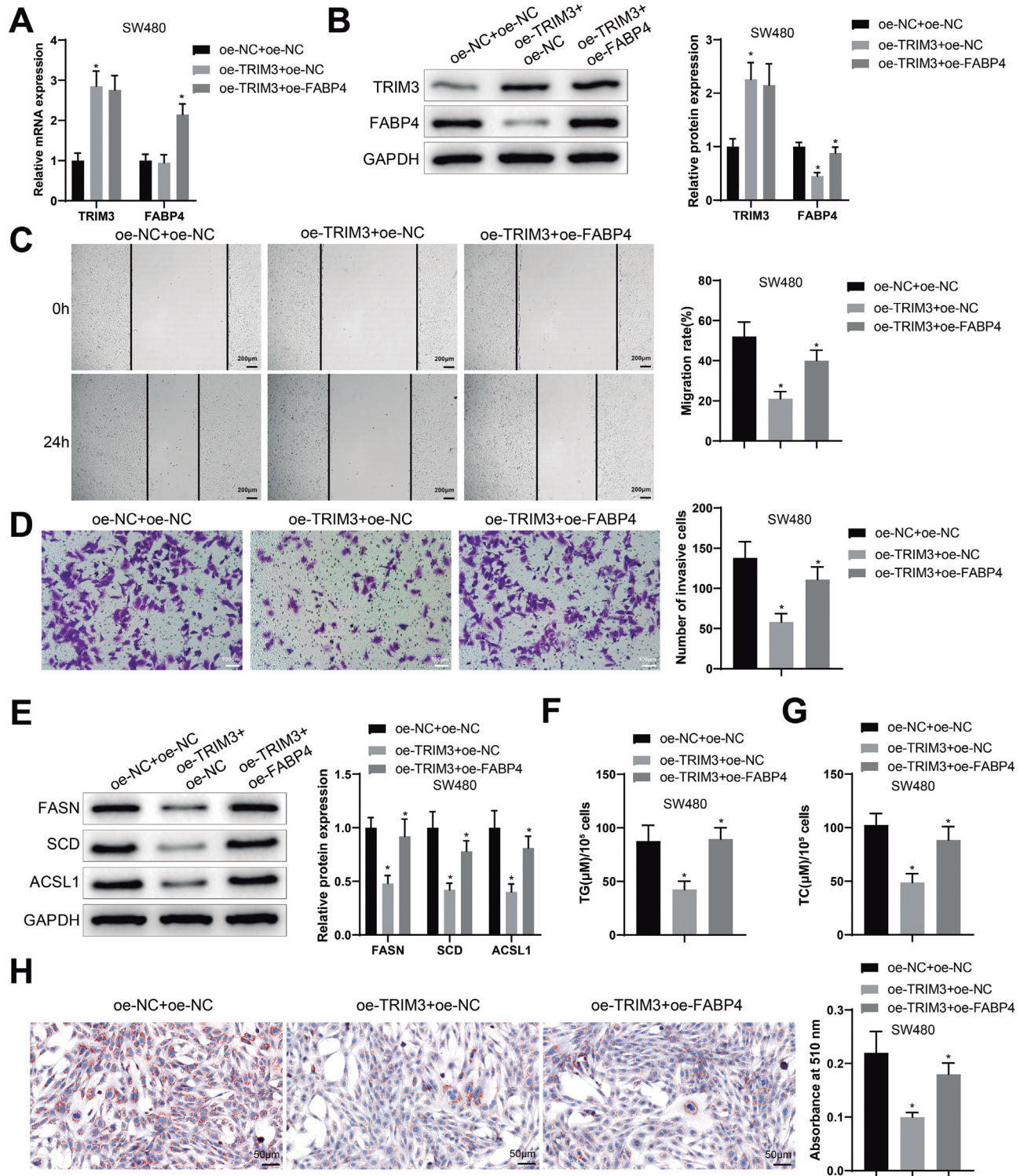


**Fig. 6.** TRIM3 modulates cell migration and the formation of LD in SW480 cells via FABP4. After SW480 cells were transfected with oe-TRIM3 or co-transfected with oe-TRIM3 and oe-FABP4. **A.** The mRNA levels of TRIM3 and FABP4 were tested by qRT-PCR. **B.** The protein expression of TRIM3 and FABP4 was measured by western blot assay. **C.** SW480 cell migration was assessed using wound healing assay. **D.** SW480 cell invasion was tested using Transwell assay. **E.** The protein levels of FASN, SCD, and ACSL1 were assessed by western blot assay. **F, G.** The levels of TG and TC were tested by ELISA kits. **H.** The number of intracellular LDs was observed through oil red O staining. Data were shown in the form of mean  $\pm$  standard deviation. One-way analysis of variance was used for comparisons among multiple groups, and Tukey's test was used for post hoc multiple comparisons. All assays were repeated thrice. \*,  $P < 0.05$ . FASN, fatty acid synthase; SCD, stearyl-CoA desaturase; ACSL1, acyl-CoA synthetase long chain family member 1; TG, triglyceride; TC, total cholesterol; LD, lipid droplet.

## FABP4 promotes CRC cell migration

modulate tumor metastasis and LD formation in CRC and found that upregulation of TRIM3 repressed the protein expression of FABP4, thereby inhibiting CRC metastasis and LD production.

At first, we observed that FABP4 expression in CRC cells was prominently elevated versus normal colonic epithelial cells. Consistently, ELISA data from a published study reflected that FABP4 concentration was higher in the plasma of CRC patients than that of the normal control (Zhang et al., 2021b). Oppositely, another research by Zhao D et al. demonstrated a low expression of FABP4 in CRC (Zhao et al., 2019). Wang H et al. confirmed the discrepancy of FABP4 expression in their study on tumor microenvironment heterogeneity in CRC and guessed that this discrepancy might be due to false positives of RNA sequencing or heterogeneity between clinical tissues and cancer cells (Wang et al., 2022). As a result, the function of FABP4 in CRC needs to be explored deeply. Our data revealed that FABP4 expression was relatively higher in HCT116 and LoVo cells among the used CRC cell lines. Therefore, HCT116 and LoVo cells were first selected for assays and transfected with sh-FABP4. The experiments confirmed that the deficiency of FABP4 resulted in declined migration and invasion in HCT116 and LoVo cells and depressed tumor metastasis in mice, illustrating that FABP4 facilitates CRC metastasis. Notably, previous research revealed that FABP4 could promote fatty acid transport to increase lipid metabolism and CRC cell migration (Tian et al., 2020). Moreover, analysis from GEPIA showed that FABP4 was positively correlated with LD formation-related genes including FASN, SCD, and ACSL1, and our further experimental results suggested that FABP4 may facilitate LD formation in HCT116 and LoVo cells. As an LD-related factor, FABP4 was widely reported to affect LD formation and the progression of diseases. Reportedly, FABP4 was strongly expressed during kidney fibrosis and accelerated lipid accumulation by modulating the metabolism pathway (Chen et al., 2021a). In ovarian cancer, silencing of FABP4 by a small-interfering RNA restrained tumor metastasis and affected metabolic pathways, ultimately weakening tumor aggressiveness (Gharpure et al., 2018).

In addition, we found that TRIM3 was down-regulated in COAD and READ through bioinformatics analysis. As a tumor suppressor, low expression of TRIM3 was detected in cancers, such as glioblastoma (Chen et al., 2014), breast cancer (Li et al., 2019), gastric cancer (Fu et al., 2018), and so on. Consistently, decreased expression of TRIM3 was shown in HCT116 and LoVo cells. Further assays verified that upregulated TRIM3 significantly promoted the ubiquitination level of FABP4 and inhibited its protein expression and that TRIM3 expression was not affected by oe-FABP4 transfection in the presence of oe-TRIM3, suggesting that FABP4 was downstream of TRIM3. The TRIM protein family is one of the largest subfamilies of E3 ubiquitin ligases, and its abnormal regulation is closely related to human diseases and cancers (Venuto and

Merla, 2019). In Ewing sarcoma cells, TRIM3 negatively modulated autophagy by improving Beclin1 K48-linked polyubiquitination to increase degradation of Beclin1 (Lu et al., 2019). Moreover, Piao MY et al. affirmed that TRIM3 overexpression may inhibit tumor growth by modulating p53 protein stabilization in CRC (Piao et al., 2016). However, the importance of TRIM3 in cell metastasis and LD formation in CRC remains to be elucidated. In accordance with the above data, we speculated that TRIM3 affected CRC metastasis and LD formation through FABP4. Our data unveiled that TRIM3 upregulation reduced migration, invasion, the protein levels of N-cadherin, Vimentin, FASN, SCD, and ACSL1, the levels of TG, and TC, and the number of intracellular LDs while elevating E-cadherin protein levels in HCT116 and LoVo cells, which was nullified by further overexpressing FABP4. Considering the fact that HCT116 and LoVo cell lines are mismatch repair-deficient cells with wild-type p53 and that TRIM3 could degrade p53, we also conducted related cellular experiments in SW480 cells with p53 deletion. The data confirmed that TRIM3 overexpression diminished migration, invasion, the protein levels of FASN, SCD, and ACSL1, the levels of TG, and TC, and the number of intracellular LDs in SW480 cells, which was abrogated by further FABP4 upregulation. In conclusion, in both p53-mutant and p53-wild-type cell lines, TRIM3 inhibited FABP4 protein expression without affecting its mRNA expression through ubiquitination degradation, thus repressing the migration and LD formation in CRC cells. Nevertheless, TRIM3 may regulate CRC cell function via other pathways, and more experiments are needed in the future.

In conclusion, our findings identified a previously unappreciated role of the TRIM3/FABP4 axis in CRC metastasis and LD formation, suggesting that TRIM3 and FABP4 may serve as biomarkers for CRC metastasis and provide an alert for the treatment. While this finding is prospective, there are still lots of limitations that demand to be overcome before they can be incorporated into clinical practice. Due to the limited number of samples in this experiment, more elaborate cellular and animal experiments should be carried out in the future to obtain more data to support our conclusions. In addition, we need to study the role of the TRIM3/FABP4 regulatory axis in the animal environment and the regulation of other target genes in CRC more comprehensively.

---

*Acknowledgements.* We acknowledge Dixian Luo (Department of Laboratory Medicine, Huazhong University of Science and Technology Union Shenzhen Hospital (Nanshan Hospital), Nanshan Avenue, Shenzhen, Guangdong, China) for her valuable advice. We acknowledge Hui Chen (Department of Pathology, The First Hospital of Changsha City, Changsha, China) for her support.

*Funding.* Thanks for the grant from the Science and Technology Department of Hunan Province (No. 2021SK53102).

*Declaration of interest.* The authors declare there is no conflict of interests.

---

**References**

- Baczewska M., Supruniuk E., Bojczuk K., Guzik P., Milewska P., Kononczuk K., Dobroch J., Chabowski A. and Knapp P. (2022). Energy substrate transporters in high-grade ovarian cancer: Gene expression and clinical implications. *Int. J. Mol. Sci.* 23, 8968.
- Chen G., Kong J., Tucker-Burden C., Anand M., Rong Y., Rahman F., Moreno C.S., Van Meir E.G., Hadjipanayis C.G. and Brat D.J. (2014). Human Brat ortholog TRIM3 is a tumor suppressor that regulates asymmetric cell division in glioblastoma. *Cancer Res.* 74, 4536-4548.
- Chen Y., Dai Y., Song K., Huang Y., Zhang L., Zhang C., Yan Q. and Gao H. (2021a). Pre-emptive pharmacological inhibition of fatty acid-binding protein 4 attenuates kidney fibrosis by reprogramming tubular lipid metabolism. *Cell Death Dis.* 12, 572.
- Chen Y., Zheng X. and Wu C. (2021b). The role of the tumor microenvironment and treatment strategies in colorectal cancer. *Front. Immunol.* 12, 792691.
- Dekker E., Tanis P.J., Vleugels J.L.A., Kasi P.M. and Wallace M.B. (2019). Colorectal cancer. *Lancet* 394, 1467-1480.
- Fu H., Yang H., Zhang X., Wang B., Mao J., Li X., Wang M., Zhang B., Sun Z., Qian H. and Xu W. (2018). Exosomal TRIM3 is a novel marker and therapy target for gastric cancer. *J. Exp. Clin. Cancer Res.* 37, 162.
- Fujii K., Luo Y., Fujiwara-Tani R., Kishi S., He S., Yang S., Sasaki T., Ohmori H. and Kuniyasu H. (2017). Pro-metastatic intracellular signaling of the elaidic trans fatty acid. *Int. J. Oncol.* 50, 85-92.
- Gharpure K.M., Pradeep S., Sans M., Rupaimoole R., Ivan C., Wu S.Y., Bayraktar E., Nagaraja A.S., Mangala L.S., Zhang X., Haemmerle M., Hu W., Rodriguez-Aguayo C., McGuire M., Mak C.S.L., Chen X., Tran M.A., Villar-Prados A., Pena G.A., Kondetimmahalli R., Nini R., Koppula P., Ram P., Liu J., Lopez-Berestein G., Baggerly K., L S.E. and Sood A.K. (2018). FABP4 as a key determinant of metastatic potential of ovarian cancer. *Nat. Commun.* 9, 2923.
- Huang M., Narita S., Inoue T., Koizumi A., Saito M., Tsuruta H., Numakura K., Satoh S., Nanjo H., Sasaki T. and Habuchi T. (2017a). Fatty acid binding protein 4 enhances prostate cancer progression by upregulating matrix metalloproteinases and stromal cell cytokine production. *Oncotarget* 8, 111780-111794.
- Huang X.Q., Zhang X.F., Xia J.H., Chao J., Pan Q.Z., Zhao J.J., Zhou Z.Q., Chen C.L., Tang Y., Weng D.S., Zhang J.H. and Xia J.C. (2017b). Tripartite motif-containing 3 (TRIM3) inhibits tumor growth and metastasis of liver cancer. *Chin. J. Cancer* 36, 77.
- Jia W., Zhang T., Huang H., Feng H., Wang S., Guo Z., Luo Z., Ji X., Cheng X. and Zhao R. (2022). Colorectal cancer vaccines: The current scenario and future prospects. *Front. Immunol.* 13, 942235.
- Li Y., Zhu H., Wang J., Qian X. and Li N. (2019). MiR-4513 promotes breast cancer progression through targeting TRIM3. *Am. J. Transl. Res.* 11, 2431-2438.
- Li Z., Liu H. and Luo X. (2020). Lipid droplet and its implication in cancer progression. *Am. J. Cancer Res.* 10, 4112-4122.
- Li T., Tang C., Huang Z., Yang L., Dai H., Tang B., Xiao B., Li J. and Lei X. (2021). MiR-144-3p inhibited the growth, metastasis and epithelial-mesenchymal transition of colorectal adenocarcinoma by targeting ZEB1/2. *Aging (Albany NY)* 13, 17349-17369.
- Liu D., Chen C., Cui M. and Zhang H. (2021). MiR-140-3p inhibits colorectal cancer progression and its liver metastasis by targeting BCL9 and BCL2. *Cancer Med.* 10, 3358-3372.
- Lu Q., Zhang Y., Ma L., Li D., Li M., Liu P. and Li J. (2019). TRIM3 negatively regulates autophagy through promoting degradation of beclin1 in ewing sarcoma cells. *Onco. Targets Ther.* 12, 11587-11595.
- Mandl M., Viertler H.P., Hatzmann F.M., Brucker C., Grossmann S., Waldegger P., Rauchenwald T., Mattesich M., Zwierzina M., Pierer G. and Zwierschke W. (2022). An organoid model derived from human adipose stem/progenitor cells to study adipose tissue physiology. *Adipocyte* 11, 164-174.
- Piao M.Y., Cao H.L., He N.N., Xu M.Q., Dong W.X., Wang W.Q., Wang B.M. and Zhou B. (2016). Potential role of TRIM3 as a novel tumour suppressor in colorectal cancer (CRC) development. *Scand. J. Gastroenterol.* 51, 572-582.
- Siegel R.L., Miller K.D., Fuchs H.E. and Jemal A. (2021). Cancer statistics, 2021. *CA Cancer J. Clin.* 71, 7-33.
- Sun N. and Zhao X. (2022). Therapeutic implications of FABP4 in cancer: An emerging target to tackle cancer. *Front. Pharmacol.* 13, 948610.
- Tian W., Zhang W., Zhang Y., Zhu T., Hua Y., Li H., Zhang Q. and Xia M. (2020). FABP4 promotes invasion and metastasis of colon cancer by regulating fatty acid transport. *Cancer Cell Int.* 20, 512.
- Tsakogiannis D., Kalogera E., Zagouri F., Zografos E., Balalis D. and Bletsas G. (2021). Determination of FABP4, RBP4 and the MMP-9/NGAL complex in the serum of women with breast cancer. *Oncol. Lett.* 21, 85.
- Venuto S. and Merla G. (2019). E3 ubiquitin ligase TRIM proteins, cell cycle and mitosis. *Cells* 8, 510.
- Walther T.C., Chung J. and Farese R.V., Jr. (2017). Lipid droplet biogenesis. *Annu. Rev. Cell Dev. Biol.* 33, 491-510.
- Wang H., Li Z., Ou S., Song Y., Luo K., Guan Z., Zhao L., Huang R. and Yu S. (2022). Tumor microenvironment heterogeneity-based score system predicts clinical prognosis and response to immune checkpoint blockade in multiple colorectal cancer cohorts. *Front. Mol. Biosci.* 9, 884839.
- Zhang Y., Zhao X., Deng L., Li X., Wang G., Li Y. and Chen M. (2019). High expression of FABP4 and FABP6 in patients with colorectal cancer. *World J. Surg. Oncol.* 17, 171.
- Zhang N., Ng A.S., Cai S., Li Q., Yang L. and Kerr D. (2021a). Novel therapeutic strategies: Targeting epithelial-mesenchymal transition in colorectal cancer. *Lancet Oncol.* 22, e358-e368.
- Zhang Y., Zhang W., Xia M., Xie Z., An F., Zhan Q., Tian W. and Zhu T. (2021b). High expression of FABP4 in colorectal cancer and its clinical significance. *J. Zhejiang Univ. Sci. B* 22, 136-145.
- Zhao D., Ma Y., Li X. and Lu X. (2019). MicroRNA-211 promotes invasion and migration of colorectal cancer cells by targeting FABP4 via PPAR $\gamma$ . *J. Cell Physiol.* 234, 15429-15437.